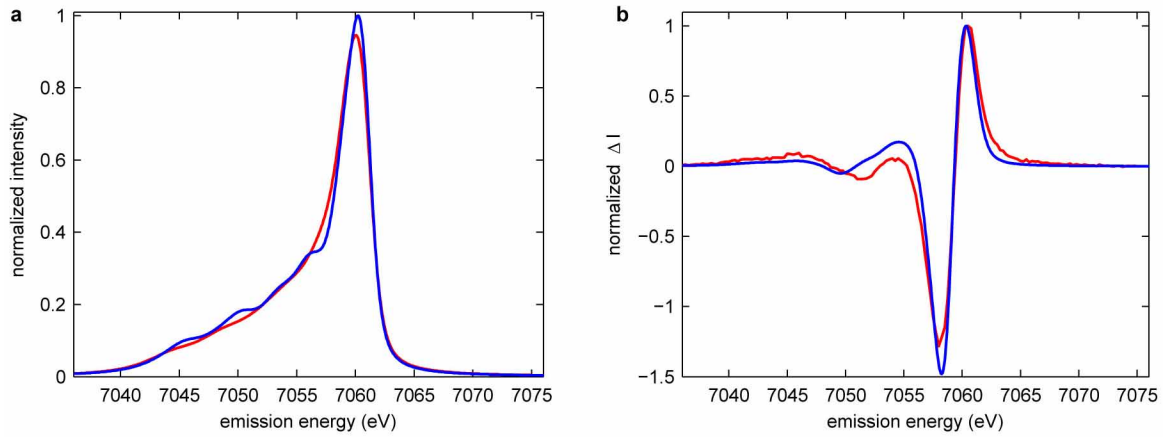

Extended Data Figure 1 | Experimental and calculated Kβ fluorescence spectra for triplet spin states. a, The calculated Kβ fluorescence spectra of iron complexes: triplet Fe(II) in square planar crystal field (red) (calculation parameters based on Fe(II)phthalocyanine), and triplet excited state in an octahedral crystal field (blue) (calculation parameters based on $[Fe(2,2'\text{-bipyridine})_3]^{2+}$). **b**, The experimental Kβ fluorescence difference spectrum (red) obtained by subtracting the singlet $[Fe(2,2'\text{-bipyridine})_3]^{2+}$ spectrum from the triplet Fe(II)phthalocyanine spectrum, and the calculated Kβ fluorescence difference spectrum (blue) generated by subtracting the spectrum of the singlet state in an octahedral crystal field from the triplet state in a square planar crystal field.

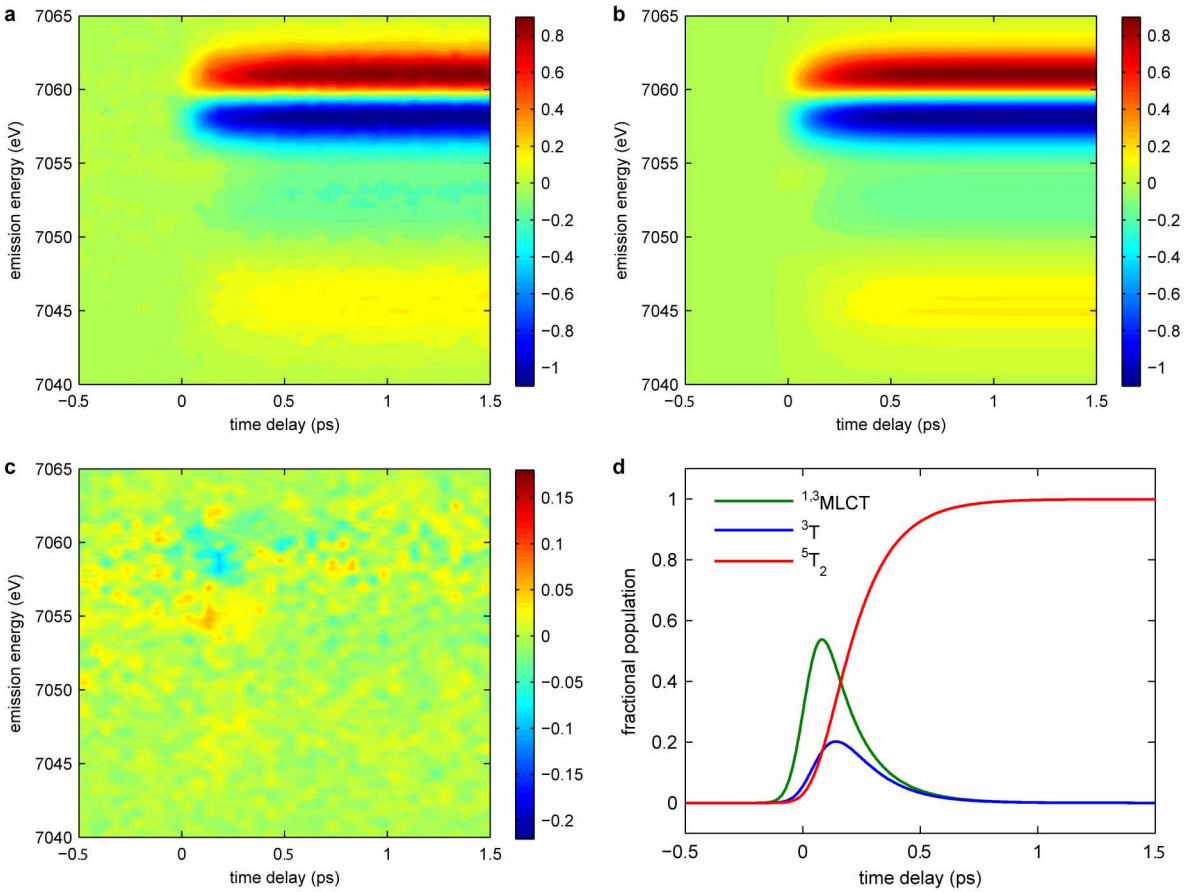

Extended Data Figure 2 | Time-dependent Kβ fluorescence spectra and fit using the sequential kinetic model with a triplet transient. **a**, Experimental transient fluorescent amplitude difference spectra plotted with arbitrary units, and **b**, fit using the sequential kinetic model with a triplet transient. **c**, Residuals for the best fit, with the colour-scale maximum and minimum set to one-fifth of the value used in **a** and **b**. **d**, The excited state populations extracted from the best fit.

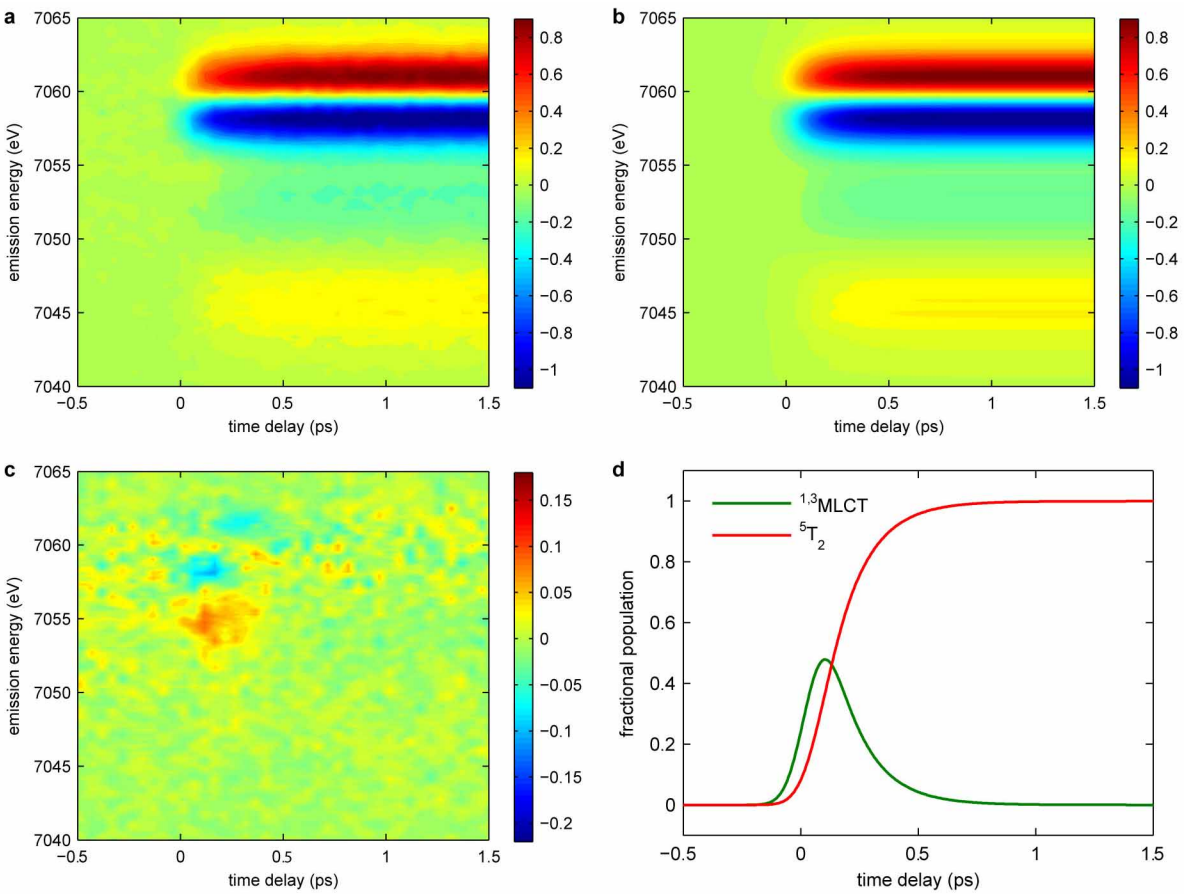

Extended Data Figure 3 | Time-dependent Kβ fluorescence spectra and fit using the direct kinetic model without a triplet transient. **a**, Experimental transient fluorescent amplitude difference spectra plotted with arbitrary units, and **b**, fit using the direct kinetic model without a triplet transient. **c**, Residuals for the best fit with the colour scale maximum and minimum set to one-fifth of the value used in **a** and **b**. **d**, The excited state populations extracted from the best fit.

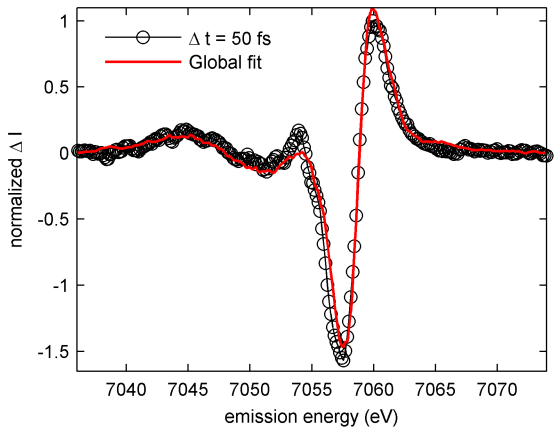

Extended Data Figure 4 | The 50 fs time delay normalized Kβ fluorescent amplitude difference spectrum (Δ*I*) and kinetic model fit plotted as a function of X-ray emission energy. The measured data (black circles and line), along with the best global fit from the sequential kinetic model with a transient triplet state (red line).

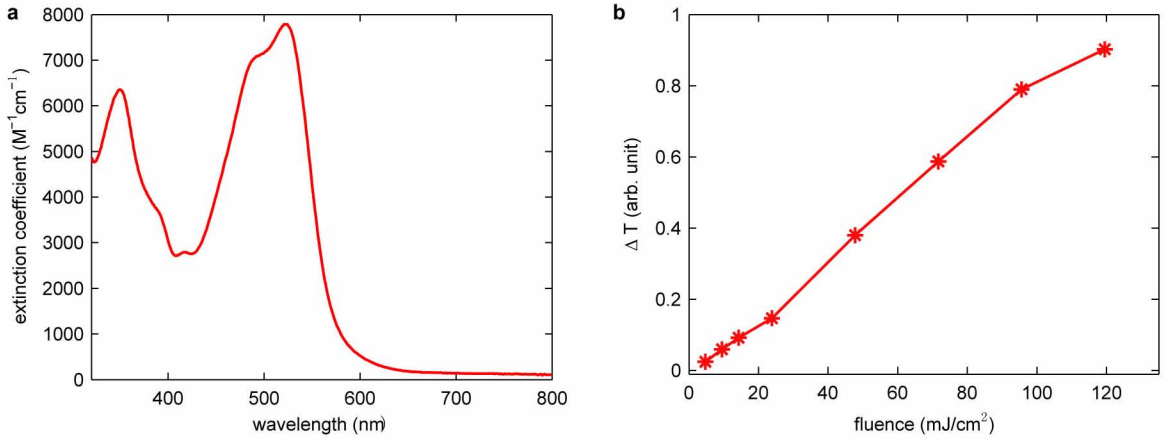

Extended Data Figure 5 | Absorption spectrum and pump power dependence measurements. **a**, The ultraviolet–visible absorption spectrum of $[Fe(2,2'\text{-bipyridine})_3]^{2+}$ in water. **b**, Power (fluence) dependence of the change in probe transmission measured at 520 nm, following excitation of an aqueous solution of $[Fe(2,2'\text{-bipyridine})_3]Cl_2$ with a 520 nm pump pulse. The figure shows the change in transmission (ΔT) measured at a 10 ps time delay, a time long compared to the spin crossover and vibrational cooling timescales, but short compared to the lifetime of the high-spin excited state.

Extended Data Table 1 | Fitted model parameters

Kinetic model	lifetime	lifetime	Time zero	Instrument response	
	$1/k_1$(fs)	$1/k_2$(fs)	t_0(fs)	σ(fs)	FWHM(fs)
with triplet transient	150±50	70±30	0±7	56±8	130±20
without triplet transient	140±12		15±6	70±7	170±15

Values shown are extracted from fits to sequential and direct spin crossover models for photo-excited $[Fe(2,2'\text{-bipyridine})_3]^{2+}$ in water. We compute the time constants and uncertainties by fitting six runs of the same experiment and then calculating the mean and standard deviation.